General Impact Factor (GIF): 0.875
Scientific Journal Impact Factor: 1.205

e- ISSN: 2394-5532
p- ISSN: 2394-823X

International Journal of Applied And Pure Science and Agriculture

www.ijapsa.com

OPTICAL STUDY ON NANOSIZED EUROPIUM DOPED $Sr_{0.5}Ba_{0.5}Nb_2O_6$ CERAMICS

Nuja J.[1], and Nandakumar K.[1,2]

[1]**Assistant Professor, CMS College,** ***School of Pure and Applied Physics,*** [2]***Centre for Nanoscience and Nanotechnology, Mahatma Gandhi University, Kottayam-686 560, Kerala, India***

Abstract

The nanosized pure and europium doped $Sr_{0.5}Ba_{0.5}Nb_2O_6$ ceramic systems have been synthesized by an aqueous organic gel route. The systems have been characterized for their structure by XRD. Particle morphology and size of the powder has been examined using SEM and TEM. The transmission electron microscopy images illustrate that the pure system powders consist of spherical particles with average size of 45 nm and europium doped system powders consist of nano rods with average size of 25 nm. Under UV light excitation, the $Sr_{0.5}Ba_{0.5}Nb_2O_6$ ceramic powder exhibited a blue emission band with a maximum at 440 nm. By doping with Eu^{3+}, orange red emitting phosphor rods can be realized. Luminescence measurements of europium doped system are assigned to the 4f-4f transitions of europium ions in the Strontium Barium Niobate host lattice. The nonlinear absorption behavior of nanosized europium doped Strontium Barium Niobate ceramic system has been investigated employing the open aperture Z-scan experiment using 532 nm, 5 ns laser pulses.

I. INTRODUCTION

Rare earth doped ultrafine and nanocrystalline oxide materials have been widely investigated due to their optical properties, which make them promising candidates for applications in optoelectronic devices and flat panel displays or in thin films-based detectors [1, 2]. Research has been particularly active for oxide systems mainly doped with the technologically important Eu^{3+} ions as a luminescent structural probe [3, 4]. Strontium Barium Niobate (SBN) is a promising photorefractive crystal widely used in optical information processing, optical computing and optical network system [5]. The optical spectroscopy of SBN powders doped with Eu^{3+} has been extensively studied [6, 7]. The formation of Eu^{3+} doped SBN have previously been prepared by different methods such as solid state reaction method, coprecipitation [8], PLD [9], and sol-gel [10-13]. Among these methods, the sol-gel route has been intensively studied because in general, this process is flexible enough to produce ceramic powders, fibers, and monoliths, as well as advantageously elaborate films of complex oxides [14-16]. Since the dopant gives rise to suitable spectroscopic properties to this kind of scintillator material, the dopant distribution into nanoparticle sites plays a major role in the development of nanoparticles based devices. The aim of the present work is the preparation of Eu^{3+} doped $Sr_{0.5}Ba_{0.5}Nb_2O_6$ nanoparticles using a novel approach by the aqueous organic gel method and to study their structural properties as well as their linear and nonlinear optical properties.

The general formula of the tungsten bronze structure is $(A_1)_2(A_2)_4C_4(B_1)_2(B_2)_8O_{30}$, where A_1, A_2, B_1, B_2 and C sites can be filled by different valence cations or may be partially empty. One unit cell consists of ten BO_6 octahedra linked by their corners to form three types of tunnels along the c axis of crystals, which are the A_1, A_2 and C tunnels corresponding to 15-, 12- and 9-fold oxygen coordinated

lattice sites. Both B_1 and B_2 are 6 fold sites located inside the BO_6 oxygen octahedral units. In the case of SBN, only five of the six available A_1 and A_2 sites are occupied by Sr^{2+} and Ba^{2+} cations on an average. B_1 and B_2 sites are completely filled with Nb^{5+} cations while C sites are empty. The partially filled structure of SBN provides large possibilities to accommodate various dopants from transition metal ions to rare earth ions.

II. EXPERIMENTAL

The starting materials used for the preparation of pure SBN and SBN: Eu^{3+} were Ba $(NO_3)_2$, Sr $(NO_3)_2$, Nb_2O_5, Eu $(NO_3)_2$, EDTA, ammonia solution and citric acid. Citric acid and EDTA were used as chelating agents. For the preparation of Ba-EDTA and Sr-EDTA complexes, barium nitrate and strontium nitrate were separately dissolved in deionised water and mixed with aqueous EDTA. The required amount of ammonia solution was added to achieve pH > 7 to form transparent Ba-EDTA and Sr-EDTA complexes. The pH of the solution was then adjusted to 7 by using nitric acid. The procedure followed for the preparation of SBN has been reported previously [17]. For the preparation of Eu^{3+} doped SBN ceramic powders stoichiometric amounts of Ba-EDTA, Sr-EDTA, Nb-citrate solutions and Europium nitrate of 2 wt. % were mixed together, followed by addition of citric acid in the molar ratio of citric acid: Nb = 3:1. The pH was adjusted to 8 by addition of ammonia solution. A clear transparent SBN: Eu^{3+} precursor solution was obtained. This solution was heated at 80°C for 24 hrs to produce a gelatinous precursor, which was then calcined at 800°C for 6 hrs in air to form the SBN: Eu^{3+} nanoceramic powders.

The FTIR spectra of the samples were taken and the formation of SBN phase have been confirmed. Thermogravimetry (TG) and differential thermal analysis (DTA) techniques were used to determine the weight loss and changes associated with phase transitions in SBN during thermal evolution and confirmed the formation of SBN nanosystem at 800°C. The XRD [X'pert PRO X-ray Diffractometer, λ=0.1541nm] data of the samples indicate the formation of SBN structure. The detailed micro structural analysis were performed using SEM [JEOL JSM 6390] and HRTEM [JEOL JEM 3010] to determine the morphology, particle size and crystallographic planes. The photoluminescence analysis were performed using a spectrofluorophotometer (Shimadzu RF-PC 5301) utilized to confirm the Europium complex formation in the host.

The open aperture z-scan [18] experiment was used to characterize the nonlinear transmission of the prepared samples. The samples were suspended in ethylene glycol by sonication and were taken in 1 mm cuvettes for the measurements. Nanosecond laser pulses from a frequency doubled Q-switched ND:YAG laser (Quanta Ray - SpectraPhysics) were used for the measurements. The propagation direction of the exciting laser is considered as the z-axis. The beam is focused using a plano-convex lens and the focal point is taken as z = 0. The beam has maximum energy density at the focus, which will symmetrically reduce towards either side of it on the z-axis. In the experiment, the sample is placed in the beam at different positions with respect to the focus (i.e, scanned on the z-axis), and the corresponding transmissions are recorded. The position Vs transmission curve thus obtained is known as the open aperture z-scan curve and from this curve the nonlinear absorption coefficient of the sample can be calculated.

III. RESULTS AND DISCUSSION

The XRD pattern of pure SBN and SBN: Eu^{3+} calcined at 800°C are shown in Fig. 1 and confirms the formation of desired phase of the prepared sample through the assigned peaks according to

JCPDS card N-39-0265. The crystallite size using the Scherrer equation and the lattice constants in heat treated powders of pure SBN and SBN: Eu^{3+} were calculated and are given in Table.1.

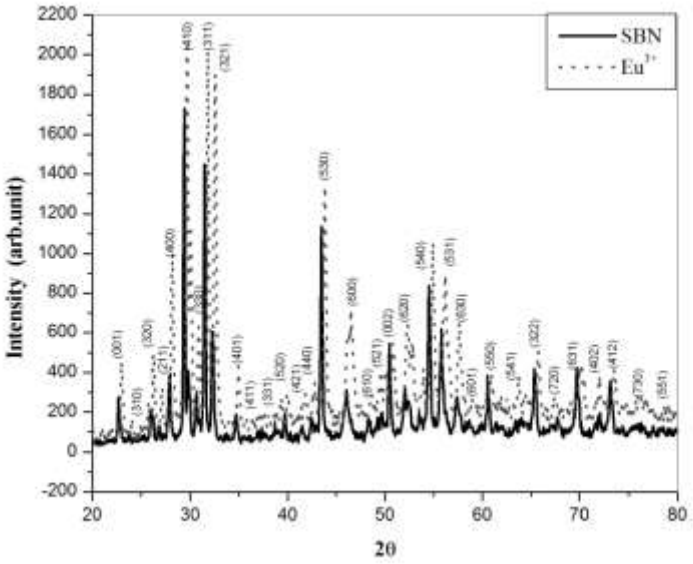

Fig. 1. XRD of pure SBN and SBN: Eu^{3+}

Table. 1. Crystallite size and Lattice constants of the samples.

Sample	Crystallite size (nm)	Lattice constants (A^0)		
		a	b	c
Pure SBN	40	12.140	12.159	3.888
SBN: Eu^{3+}	32	12.426	12.342	4.069

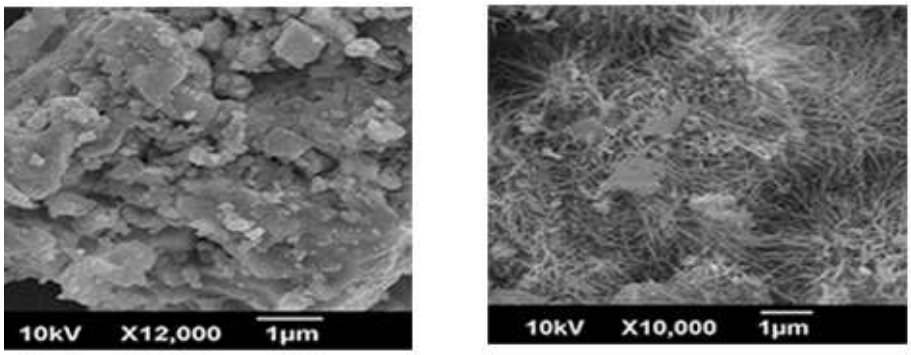

Fig. 2. SEM of pure SBN and SBN: Eu^{3+}

The SEM micrograph of pure SBN is shown in Fig. 2 and the microstructure observation shows grain size to be 0.1 to 3 micrometer and the image of SBN: Eu^{3+} system indicates the morphology of nanowires revealing the strong influence of Eu^{3+} ions on the SBN microstructure [19].

The bright field TEM of pure SBN and SBN: Eu^{3+} for metal carboxylate gel derived powders heated at 800^0C are shown in Fig. 3. The transmission electron microscopy image illustrate that the SBN powders consist of spherical monocrystalline nanoparticles with size ranging from 25 to 50 nm. The basic morphology in the europium doped SBN ceramic system are nanorods with the average crystallite diameter of 25nm and length 166nm. The selected area electron diffraction pattern in Fig. 4 confirms that SBN: Eu^{3+} nanorods mainly consist of polycrystalline material. The corresponding lattice fringe image of the europium doped SBN ceramic system analysed the spacing of sets parallel fringes 0.27, 0.32 and 0.34 nm which corresponds to crystallographic planes (311), (410) and (330).

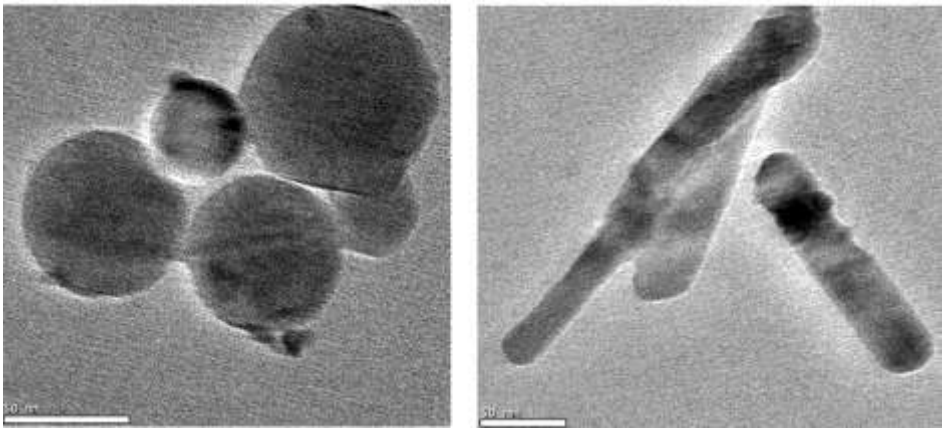

Fig. 3. TEM images of pure SBN and SBN: Eu^{3+} system

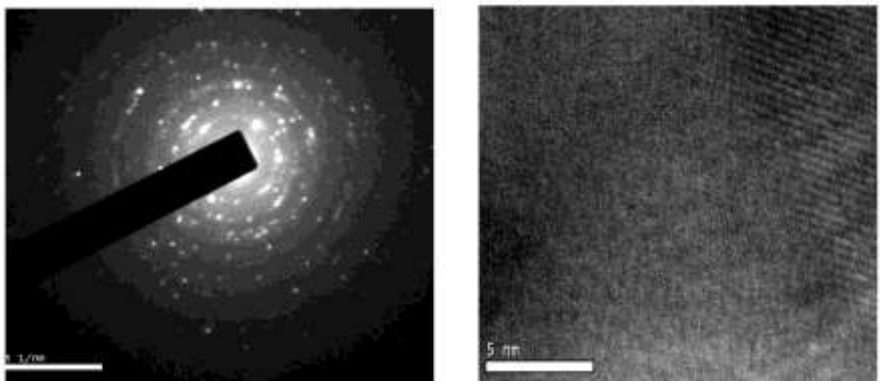

Fig. 4. Selected electron diffraction pattern and Lattice fringe image of SBN: Eu^{3+}

The emission as shown in Fig. 5 from undoped SBN ceramic system was observed by excitation at 355nm in UV region using a Xenon lamp as excitation source is attributed to charge transfer vibronic excitons (CTVE). Upon excitation, charge carriers are produced in the conduction band. They are trapped

at a niobium center to form quadravalent Nb^{4+}, leaving holes behind in the valence band [8]. Such induced charge transfer vibronic excitons in ferroelectric SBN solid solutions are considered to be the origin of the observed emission at 440nm. The charge transfer occurs between oxygen and niobium ions accompanied by self consistent lattice distortion. The CTVE electric dipole and soft TO phonon interaction as well as Jahn Teller type of interactions play an important role in lowering CTVE energy [20].

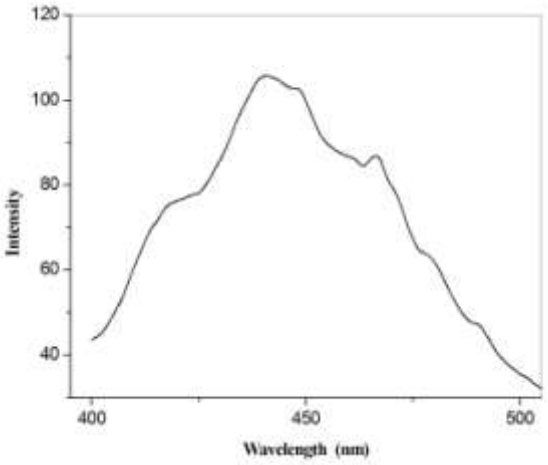

Fig. 5. Emission spectrum of SBN

Fig. 6 shows the room temperature excitation spectrum and emission spectrum of SBN: Eu^{3+} ceramic system. The intense peaks at 401, 448, 472 and 484 nm correspond to $^7F_0$–$^5L_6$, $^7F_0$–$^5D_1$, $^7F_0$–$^5D_2$ and $^7F_0$–$^5D_3$ transitions respectively. The orange red emission from the system is easily seen to the naked eye when excited with 448 nm from UV lamp. When excited at 448nm wavelength, the weak sharp peak observed at 528, 558, 580 and two unresolved emission peaks at 597nm and 603nm are due to the intra-4f transitions of Eu^{3+} ions and corresponds to the magnetic dipole transition $^5D_0 \rightarrow {}^7F_1$ and and the electric dipole transition, $^5D_0 \rightarrow {}^7F_2$ respectively. The ratios of the intensity of 603 nm emission ($^5D_0 \rightarrow {}^7F_2$) to that of 590 nm emission ($^5D_0 \rightarrow {}^7F_1$) suggest that Eu^{3+} ions are located in a more asymmetric environment for the sol–gel-derived phosphors [21].

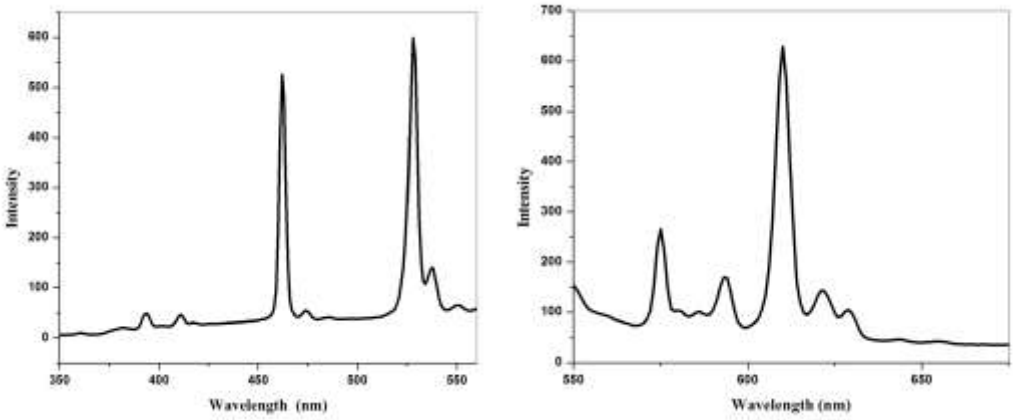

Fig. 6. Excitation and emission spectrum of SBN: Eu^3

Our automated z-scan setup used a precision stepper motor controlled translation stage to move the sample along the z- direction. The sample was translated along the beam axis through the focal region over a distance substantially longer than the Rayleigh range. The sample suspensions were prepared such that all of them had the same linear transmittance of 70% at the excitation wavelength of 532 nm. Two pyroelectric energy probes (Rj7620, Laser Probe Inc.) were used to monitor the input and transmitted energies through the sample. The temporal pulse width of the laser pulses was 7 nanoseconds (FWHM). The pulses were fired in the "single shot" mode, allowing sufficient time between successive pulses to avoid accumulative thermal effects in the sample.

Since the sample sees different laser intensities at each position, this position dependent transmission can be easily scaled to its intensity dependent transmission. For instance, for an incident Gaussian beam of wavelength λ, the beam radius at position z is given by $\omega(z)= \omega(0)[1+(z/z_0)^2]^{1/2}$ where $\omega(0)$ is the focal spot radius and z_0 is the Rayleigh range given by $\pi\,\omega(0)^2/\lambda$. Therefore knowing the energy of the input laser pulse, the input laser fluence and intensity can be calculated for each z value. The nonlinear transmission curves obtained from the z-scan measurements are given in Fig. 7.

It is seen that a 3-photon absorption (3PA) type process gives the best fit to the obtained experimental data. The z-scan curve obtained is therefore numerically fitted to the nonlinear transmission equation for a three-photon absorption process [22] given by

$$T = \frac{(1-R)^2 \exp(-\alpha L)}{\sqrt{\pi}\, p_0} \int_{-\infty}^{+\infty} \ln\left[\sqrt{1+{p_0}^2 \exp(-2t^2)} + p_0 \exp(-t^2)\right] dt \qquad (1)$$

where T is the transmission of the sample, R is the Fresnel reflection coefficient at the sample-air interface, α is the linear absorption coefficient, and L is the sample length. p_0 is given by $[2\gamma(1-R)^2 I_0^2 L_{eff}]^{1/2}$ where γ is the three-photon absorption coefficient, and I_0 is the incident intensity. L_{eff} is given by $[1- \exp(-2\alpha L)]/2\alpha$. The calculated value for the effective three-photon absorption coefficient for SBN is 2.8 x 10^{-24} m^3/W^2 [23] and that for SBN: Eu^{3+} is 3.2 x 10^{-25} m^3/W^2. Since the sample has some absorption at the excitation wavelength the observed three photon absorption is not a genuine one which involves virtual states; rather the actual physical process here is reverse saturable absorption (RSA), which involves more than one real excited state. Moreover, nanosecond laser pulses of moderate energies generally cannot provide sufficient irradiance for the occurrence of a genuine 3PA process. Therefore, the three photon absorption coefficients calculated here should be considered as effective 3PA coefficients.

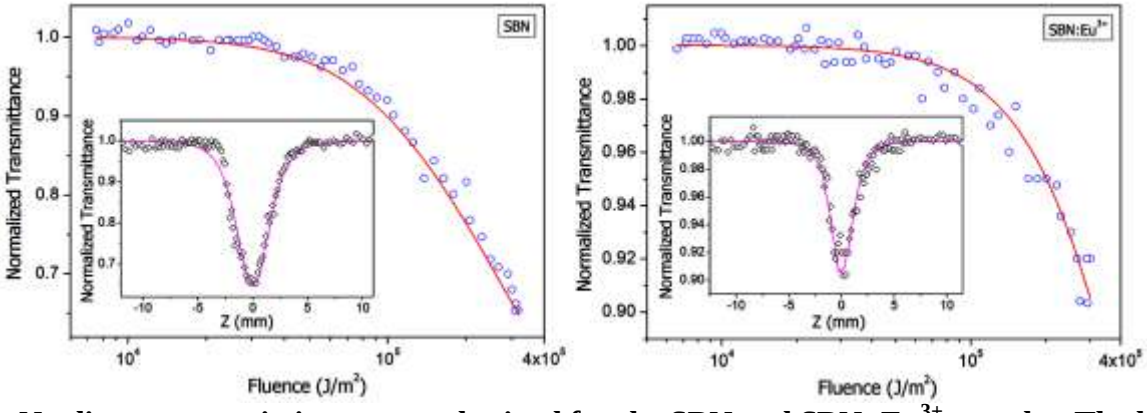

Fig. 7. Nonlinear transmission curves obtained for the SBN and SBN: Eu^{3+} samples. The hollow hexagons are data points and the solid curve is the corresponding three-photon fit to the data. Insets show the Z-scan curves.

IV. CONCLUSIONS

The pure SBN and SBN: Eu^{3+} ceramic nanosystems were prepared through an aqueous gel method. The XRD analysis confirms tungsten bronze structure. The microstructure was examined by SEM, and TEM images identified the particle size in nanometer range. A broad band emission in the UV region extending to the visible was observed following excitation at 355nm for undoped SBN. This emission is attributed to exciton luminescence of undoped SBN ceramic system. The bright red orange emission peaks at 597nm and 603nm have been observed when excited at 448nm for SBN: Eu^{3+} ceramic nanoparticles due to the 4f - 4f transitions of Eu^{3+} ions. The nonlinear absorption behavior was investigated employing the open aperture z-scan experiment using 532 nm, 5 ns laser pulses. A cascaded three-photon absorption involving real energy states is observed, and an effective three-photon absorption coefficient of $2.8x10^{-24}$ m^3/W^2 and 3 x 10^{-25} m^3/W^2 have been numerically calculated for SBN and SBN: Eu^{3+} ceramic systems respectively. This indicates that SBN and SBN: Eu^{3+} can be potential candidates for optical limiting applications. This novel and efficient pathway could open new opportunities for further investigating the novel properties of tungstate materials. The strong visible-light emission, generated from the entire doped nanorods is expected to have many applications in nanosized lighting sources and nanospectroscopy.

BIBLIOGRAPHY

[1] Battisha. K et al., structural and optical studies of activated thin film and monolith nano-structure silica gel with different rare earth elements prepared by sol-gel techniques, Indian J. Pure Appl. Phys. 2007, 45, 441-453
[2] Tissue. B.M. et al., Synthesis and luminescence of lanthanide ions in nanoscale insulating hosts, Chem. Mater. 1998, 10, 2837-2845.
[3] Margarita García-Hernández et al.,Eu-Doped $BaTiO_3$ Powder and Film from Sol-Gel Process with Polyvinylpyrrolidone Additive, Int. J. Mol Sci. 2009, 10 (9) 4088–4101.
[4] Honghua Huang and Bing Yan , Sol-gel synthesis of $Y_xGd_{2-x}SiO_5:Eu^{3+}$ phosphors derived from the in situ assembly of multicomponent hybrid precursors, Optical Materials, 2006, 28 (5), 556-559.
[5] M. J. Moghimi H, G. Fard. A and Rostami Multiwavelegths Optical Switching and Tunable Filters Using Dynamic Superimpose Photorefractive Bragg Grating, Progress In Electromagnetics Research C, 2008, 3, 129–142.
[6] H. Liu et al., Optical property of Eu in strontium barium niobate optical thin film grown by pulsed laser deposition, Thin Solid Films, 2003, 424, 61–65.
[7] A. Andresen et al., Spectroscopy of Eu^{3+} ions in congruent strontium barium niobate crystals, Physical Review B, 2008, 77, 214102.
[8] H. Liu et al., Non linear optical dynamics and Eu^{3+} spectral hole burning in strontium barium niobate optical thin film grown by pulsed laser deposition, J.Appl. Phys. 2002, 91, 129.
[9] Liu H et al., Optical properties of undoped and Eu^{3+}-doped SBN thin film grown by pulsed laser deposition, J. of luminescence 1999, 83-84, 367-371.
[10] Dong Gun Lee et al., Ferroelectric Properties of SBN Thin Films Deposited by Ion Beam Sputtering, Ferroelectrics, 2004, 304 (1), 173 – 177.
[11] Junmo Koo et al., Optical and Electrical Properties of Ferroelectric SBN Thin Films prepared by Sol-Gel Process, Journal of Sol-Gel Science and Technology, 2000, 19, 611–614.
[12] S. B. Majumder et al., Synthesis of $Sr_{0.5}Ba_{0.5}Nb_2O_6$ (SBN) thin films by sol-gel technique, Ferroelectrics, 2000, 241 (1) , 287 – 294.
[13] Jiupeng Zhao et al., Preparation and electrical properties of SBN thin films derived from aqueous organic gels, Materials Letters 2004, 58, 1456– 1460.
[14] Myoung-SupKim et al., Microstructure and dielectric characteristics of tungsten bronze structured SBN70 ceramics: effect of Nb2O5 content, J. European Ceramic Society2002, (22) 2107–2113.
[15] J.J. Romero et al., Growth and characterization of Nd-doped SBN single crystal fibers, Applied Physics A: Materials Science & Processing, 2004, 78 (7) 1037-1042.

[16] Yasuhiro Shimizu, K. R. Udayakumar, L. Eric Cross, Preparation and Electrical Properties of Lanthanum-Doped Lead Titanate Thin Films by Sol–Gel Processing, 2005, 74 (12), 3023 – 3027.
[17] Yao Li ,Jiupeng Zhao, "Low temperature preparation of nanocrystalline $Sr_{0.5}Ba_{0.5}Nb_2O_6$ powders using an aqueous organic gel route, Mater. Res. Bull. 2004, 39, 365.
[18] M. Sheik- Bahae et al., IEEE, J. Quantum Electron, 1990, 26, 760.
[19] Jilin Zhanga and Guangyan Hong, Synthesis and photoluminescence of the $Y_{2O3}:Eu^{3+}$ phosphor nanowires in AAO template, J. of Solid State Chemistry, 2004, 177, (4-5),1292-1296.
[20] H.Liu, J.Reeves,R.C.Powell and L.A.Boatner, Polarisation dependence of the nonlinear optical responses of $KTa_{1-x}Nb_xO_3$ crystals after picoseconds pulse lase excitation Phys. Review B. 1994, 49, 6823.
[21] Pązik, R.; Hreniak, D.; Stręk, W.; Kessler, V.G.; Seisenbaeva, G.A. Photoluminescence investigations of Eu^{3+} doped BaTiO3 nanopowders fabricated using heterometallic tetranuclear alkoxide complexes. J. Alloys Comp. 2008, 451, 557-562.
[22] R.L. Sutherland, Handbook of Nonlinear optics, 2nd Edition, 2003, Marcel Dekker, New York (1996).
[23] Nuja J.[1], Suchand Sandeep C.S.[3], Reji Philip[3*] and Nandakumar K. (Accepted in Spectroscopy Letters)

